**NASA
Technical
Paper
2387**
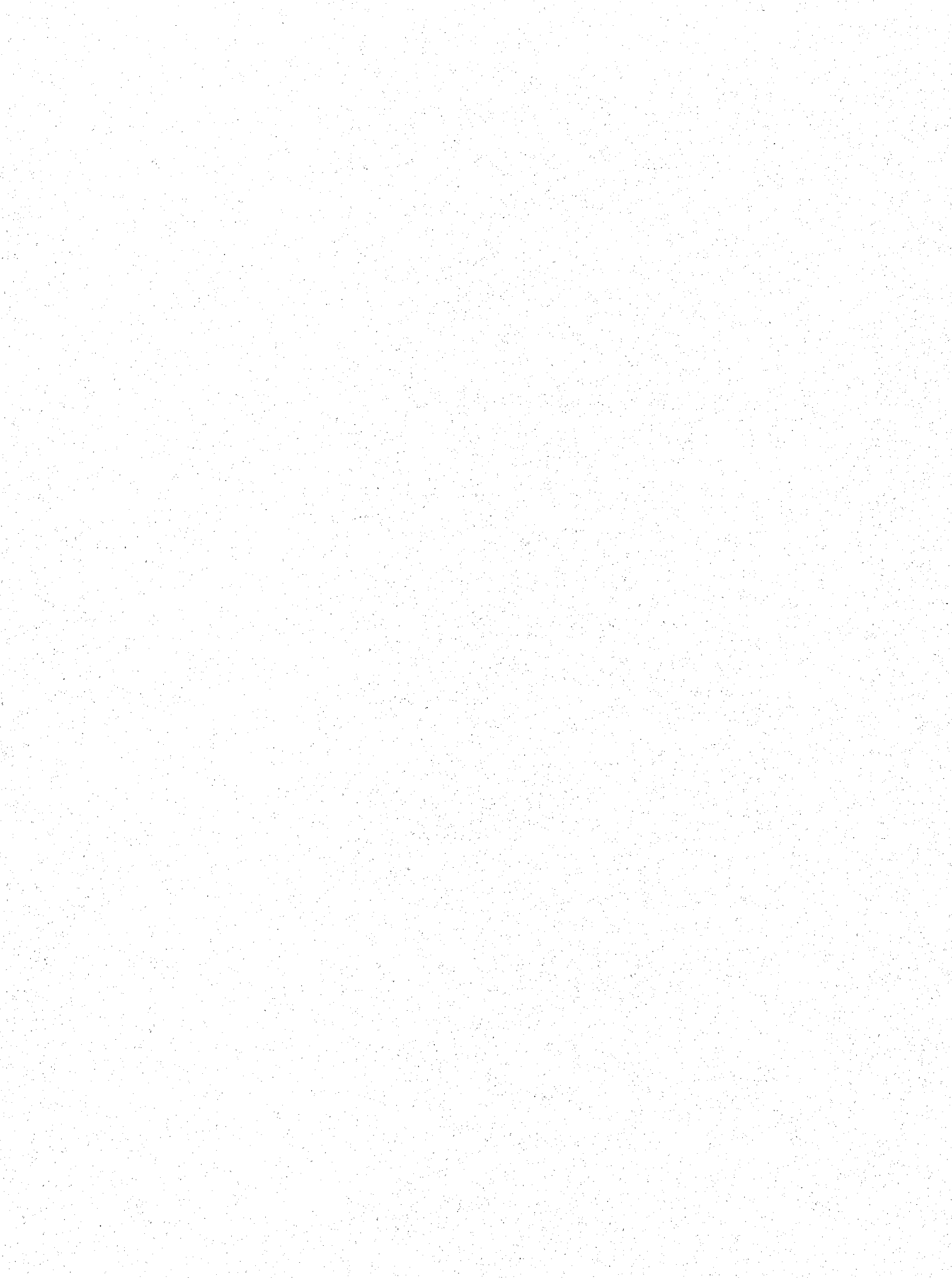
December 1984

Local Stability Analysis for a Planar Shock Wave

M. D. Salas

NASA

Local Stability Analysis for a Planar Shock Wave

M. D. Salas

Langley Research Center
Hampton, Virginia

Introduction

When solutions of the steady Euler equations are sought as solutions of a stationary problem, rather than in the limit of some temporal evolution, the solutions found may not be unique. However, not every solution of the steady equations can be expected to represent a physically meaningful flow field. A *physically meaningful* flow field is one that can be observed in nature. A physically meaningful steady flow field, in addition to satisfying the steady equations, must also be stable. A *stable* solution, in the strictest sense, represents a system which, when subjected to small finite perturbations, damps them out and returns to its original state. In mathematical terms, such a solution is known as asymptotically stable in the sense of Liapunov.

An example of a flow field with multiple solutions is shown in figure 1. The figure shows the Mach number distribution in a nozzle with an exit boundary condition such that a supersonic flow is established downstream of the sonic throat located at $x = 0$ in the figure. There are two solutions consistent with the steady equations (quasi-one-dimensional Euler equations in this case) and the given boundary conditions: one with a shock wave in the divergent section of the nozzle (curve $abcde$) and the other with a shock wave in the convergent section (curve $abfde$). It is well-known (see ref. 1) that the solution with the shock in the divergent section is stable, while the solution with the shock in the convergent section is unstable. The arguments given in most text-books (see ref. 1) to explain the instability are, however, not rigorous. The purpose of this report is to present a simple mathematical procedure to analyze the stability of flows involving planar shock waves. A *planar shock wave* here means one whose line of interception with the plane on which the solution is sought is a straight line. The mathematical procedure is based on conditions only in the immediate neighborhood of the shock, so it is therefore referred to as a "local analysis." The local analysis provides necessary conditions for stability. To establish necessary and sufficient conditions for stability, a global analysis, which takes far-field boundary conditions into account, is required. The disadvantage of the global analysis is that, in general, it requires numerical integration to solve the resulting eigenvalue problem. On the other hand, with the local analysis, a closed-form solution can be obtained.

The stability of a shock wave in the divergent-convergent section of a nozzle was studied analytically by Kantrowitz (ref. 2) in 1947, and numerically by Moretti (ref. 3) in 1971. Recently, Culick and Rogers (ref. 4) have repeated the analysis of Kantrowitz to study the response of a normal shock in a ramjet engine. Their analysis, like that of Kantrowitz is based on the assumption of quasi-steady behavior. As a justification
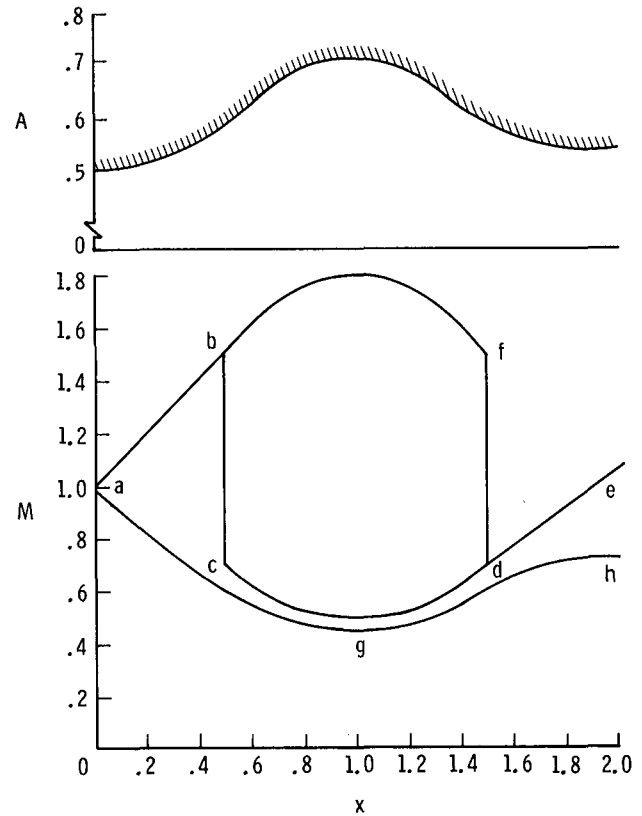

Figure 1. Nozzle flow field with two possible solutions: one corresponding to a shock in the divergent section ($abcde$) and the other corresponding to a shock in the convergent section ($abfde$).

for the quasi-steady approximation, they consider the ratio of the time derivative to the space derivative occurring in the one-dimensional continuity equation, namely

$$\frac{\frac{\partial \rho}{\partial t}}{\frac{\partial \rho u}{\partial x}} \approx \frac{\frac{\Delta \rho}{\rho u} \frac{\Delta x}{\Delta t}}{\frac{\Delta \rho}{\rho} + \frac{\Delta u}{u}} \tag{1}$$

and they assume that the characteristic length Δx over which spacial changes are significant is of the order of the shock-wave thickness. Because the shock thickness is of the order of a few mean free paths, they concluded that the time derivative may be ignored. There are two errors in this analysis. First, the ratio in equation (1) obviously has a value of -1. They should have considered the ratio of the unsteady term to one of the steady terms, not to both; for example, the ratio

$$\frac{\frac{\partial \rho}{\partial t}}{u \frac{\partial \rho}{\partial x}} \approx \frac{1}{u} \frac{\Delta x}{\Delta t} \tag{2}$$

The second, and perhaps a worse error, is that the characteristic length is not of the order of the shock-wave thickness, but rather of the order of the shock-wave excursion. Therefore, the term $\Delta x/\Delta t$ in equation (2) is

of the order of the shock speed w. The time derivatives are, therefore, of the same order as the shock speed and are retained in the present analysis.

The analysis presented here is first developed for the nozzle problem just discussed. It is then used to investigate how the stability of the shock changes if the shock is assumed to be isentropic. Finally, it is used to study the stability of weak and strong shocks attached to wedges and cones—a problem previously investigated by the author in reference 5.

Symbols

a speed of sound

A cross-sectional area of quasi-one-dimensional nozzle

c damping coefficient

F steady-state part of compatibility equation

j equal to 0 for a two-dimensional wedge and to 1 for an axisymmetric circular cone

k spring coefficient

m mass coefficient

M Mach number

p pressure

P defined by equation (17), (39), or (57)

Q defined by equation (18), (40), or (58)

r radial coordinate (fig. 7)

r_o radial coordinate at which governing equation is evaluated

R defined by equation (19), (41), or (59)

S defined by equation (20), (42), or (60)

t time in fixed frame of reference

T defined by equation (64)

u longitudinal velocity component for nozzle problem; circumferential velocity component for wedge or cone problem

v radial velocity component for wedge or cone problem

V_∞ magnitude of free-stream velocity

w shock-wave speed

x longitudinal coordinate in fixed frame of reference

z shock location relative to initial position

α defined by equation (8)

β defined by equation (14)

γ isentropic exponent

δ defined by equation (13)

ς damping ratio

θ circumferential coordinate (fig. 7)

λ characteristic slope

ξ space coordinate in moving frame of reference

ρ density

τ time coordinate in moving frame of reference

ω undamped natural frequency

Subscripts:

s value at shock wave

z differentiation with respect to z

ξ differentiation with respect to ξ

τ differentiation with respect to τ

0 value at $t = 0$

1 low-pressure side of shock wave

2 high-pressure side of shock wave

∞ free-stream value

Superscripts:

$+$ left-running characteristic for wedge or cone problem

$-$ left-running characteristic for nozzle problem

A dot over a symbol denotes the derivative with respect to time.

Details of the Method

Nozzle Problem With Rankine-Hugoniot Shock

Consider the steady flow that develops in a nozzle as shown in figure 1. At time $t = 0$, assume that the shock is perturbed from its steady-state position by assigning to the shock some "small" velocity w_0. The ensuing evolution will be studied to determine whether the shock will return to its steady-state position. With the assumption that the flow is governed by the quasi-one-dimensional Euler equations, the solution is known exactly upstream of the shock as a function of the nozzle area. Downstream of the shock, the left-running characteristic brings information from the subsonic region to the shock, as indicated in figure 2. The shock motion is governed by the Rankine-Hugoniot jumps and by the compatibility relation reaching the shock along the left-running characteristic. In terms of space and time
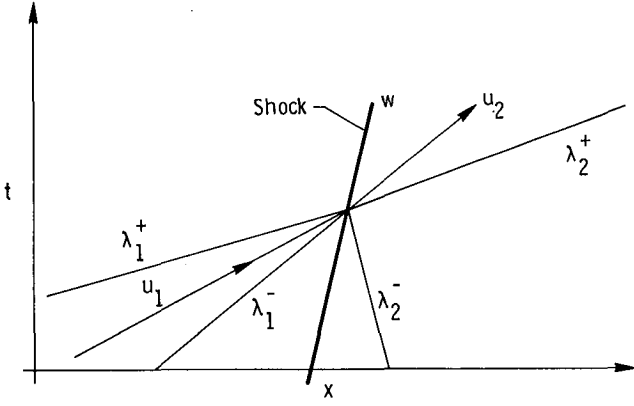
Figure 2. Characteristic diagram in the neighborhood of a shock wave.

coordinates (ξ, τ) in a frame of reference that moves with the shock,

$$
\left.\begin{array}{l}
\tau = t \\
\xi = x - x_s(t)
\end{array}\right\} \tag{3}
$$

the compatibility relation valid on the left-running characteristic is

$$
\frac{p_\tau}{p} - \gamma M \frac{u_\tau}{u} + (\lambda^- - w)\left(\frac{p_\xi}{p} - \gamma M \frac{u_\xi}{u}\right) + \gamma u \alpha = 0 \tag{4}
$$

where the shock speed is given by

$$
w = \frac{dx_s}{dt} \tag{5}
$$

and

$$
\lambda^- = u - a \tag{6}
$$

$$
M = \frac{u}{a} \tag{7}
$$

$$
\alpha = \frac{1}{A(x)}\frac{dA(x)}{dx} \tag{8}
$$

$$
a^2 = \frac{\gamma p}{\rho} \tag{9}
$$

In the above equations, (x,t) are the longitudinal and time coordinates in the fixed frame of reference; ρ, p, and a are the density, pressure, and speed of sound; u is the velocity in the longitudinal direction; γ is the isentropic exponent; x_s is the shock position; and $A(x)$ is the cross-sectional area of the nozzle.

The jump conditions connecting the supersonic side, denoted by subscript 1, to the subsonic side, denoted by subscript 2, are

$$
\frac{p_2}{p_1} = \frac{\gamma(M_1 - \frac{w}{a_1})^2 - \delta}{\beta} \tag{10}
$$

$$
\frac{u_2 - w}{u_1 - w} = \frac{1 + \delta(m_1 - \frac{w}{a_1})^2}{\beta(M_1 - \frac{w}{a_1})^2} \tag{11}
$$

where

$$
M_1 = \frac{u_1}{a_1} \tag{12}
$$

$$
\delta = \frac{\gamma - 1}{2} \tag{13}
$$

$$
\beta = \frac{\gamma + 1}{2} \tag{14}
$$

Equations (10) and (11) are valid along the shock path, $\xi = 0$. Therefore, by taking the derivative $\frac{\partial}{\partial \tau}|_{\xi=0}$ of these two equations, the rate of change in time of p_2 and u_2 can be related to the changes taking place on the supersonic side of the shock due to the shock motion. After performing this operation, the resulting equations are linearized by neglecting terms of order $(w/a_1)^2$ and higher. Finally, the derivatives $\partial M_1/\partial\tau, \partial p_1/\partial\tau$, and $\partial a_1/\partial\tau$ are replaced by the quasi-one-dimensional relations given in appendix A. The final expressions are

$$
\left.\frac{p_\tau}{p}\right|_2 = P\alpha w + Q w_\tau \tag{15}
$$

$$
\left.\frac{u_\tau}{u}\right|_2 = R\alpha w + S w_\tau \tag{16}
$$

where

$$
P = \frac{\gamma M_1}{1 - M_1^2}\left[M_1 - \frac{2M_2}{\beta}\left(1 + \delta M_1^2\right)\frac{a_1}{a_2}\right] \tag{17}
$$

$$
Q = \frac{-2\gamma M_2}{\beta a_2} \tag{18}
$$

$$
R = -\frac{1}{1 - M_1^2}\left[1 + 2\frac{\rho_2}{\rho_1}\left(\frac{\delta}{\beta} - \frac{\rho_1}{\rho_2}\right)\left(1 + \delta M_1^2\right)\right] \tag{19}
$$

$$
S = \frac{1}{a_2 M_2}\left[1 - \frac{\rho_1}{\rho_2} - 2\left(\frac{\delta}{\beta} - \frac{\rho_1}{\rho_2}\right)\right] \tag{20}
$$

With the aid of equations (15) and (16), equation (4) is evaluated at the shock to get

$$
(\gamma M_2 S - Q)w_\tau + \left[\gamma M_2 R - P + \frac{\frac{F}{\alpha a_2} - \gamma M_2}{M_2 - 1}\right]\alpha w - F = 0 \tag{21}
$$

where

$$F = \left[\lambda^{-} \left(\frac{p_\xi}{p} - \gamma M \frac{u_\xi}{u} \right) + \gamma u \alpha \right]_2 \qquad (22)$$

Equation (21) describes the shock motion. In the analysis of references 2 and 4, the equation describing the shock motion is obtained, somewhat arbitrarily, from one of the shock jump conditions. Equation (21), on the other hand, simultaneously accounts for the interaction of the pressure and velocity fields on the shock motion. In the steady state, $F = 0$. Considering departures from equilibrium to be small allows the term F appearing in the coefficient of w in equation (21) to be neglected. With the notation,

$$m = \gamma M_2 S - Q \qquad (23)$$

$$c = \left(\gamma M_2 R - P + \frac{\gamma M_2}{1 - M_2} \right) \alpha \qquad (24)$$

equation (21) can be written as

$$m w_\tau + c w = F \qquad (25)$$

The solution to this equation is given by

$$w(\tau) = \exp \left(- \int_0^\tau \frac{c}{m} \, dt \right)$$
$$\times \left[\int_0^\tau \exp \left(\int_0^\tau \frac{c}{m} \, dt \right) \frac{F}{m} \, dt + w_0 \right] \qquad (26)$$

If F is neglected entirely, the solution simplifies to

$$w(\tau) = w_0 \exp \left(- \int_0^\tau \frac{c}{m} \, dt \right) \qquad (27)$$

As shown subsequently, the coefficients m and c/α are positive for all values of M_1. Therefore, the shock velocity given by equation (27) grows exponentially if $\alpha < 0$ or decays exponentially if $\alpha > 0$. This proves stability in the sense of Liapunov (ref. 6).

Now, the effect of F on the motion of the shock is taken into consideration. Let z be the displacement of the shock wave from its equilibrium position,

$$z(\tau) = x_s(\tau) - x_{s,0} = \int_0^\tau w \, dt \qquad (28)$$

Since only small deviations from equilibrium are considered, F may be expanded in a Taylor series,

$$F(t) = F_\tau \tau + F_{\tau\tau} \frac{\tau^2}{2!} + \cdots \qquad (29)$$

or alternatively,

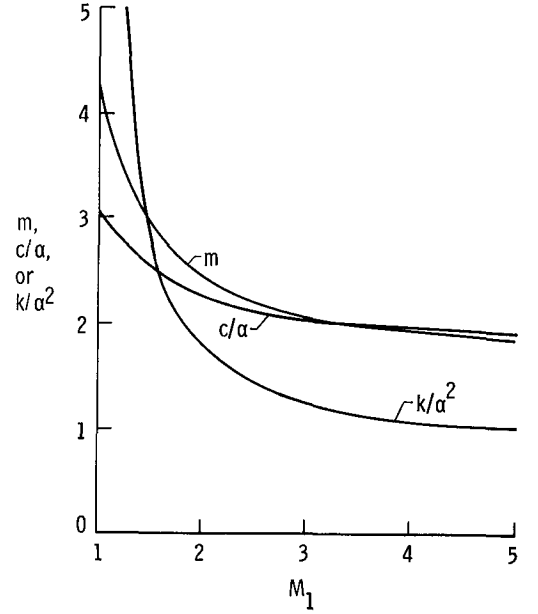$$F(z) = F_z z + F_{zz} \frac{z^2}{2!} + \cdots \qquad (30)$$

Figure 3. Behavior of $m, c/\alpha$, and k/α^2 as functions of M_1. $\gamma = 7/5$.

where the derivatives in equations (29) and (30) are, of course, evaluated at the subsonic side of the shock and $\tau = 0$ or $z = 0$. The first order, or linear, approximation to equation (25) is, therefore,

$$m\ddot{z} + c\dot{z} + kz = 0 \qquad (31)$$

where

$$k = -F_z = -\frac{F_\tau}{w_0} \qquad (32)$$

and where, to simplify the notation, a dot denotes differentiation with respect to τ. According to Liapunov's theorem (ref. 6), the information obtained from the linear approximation (i.e., eq. (31)) is sufficient to give a correct answer to the question of stability of the nonlinear equation (i.e., eq. (25)) as long as F_z is nonzero. If the coefficients of equation (31) are assumed to be constant, then the equation describes the well-known damped harmonic oscillator; see, for example, reference 7 or 8. The coefficients m, c, and k are the respective mass, damping, and spring coefficients of an equivalent oscillator. After several simplifying assumptions, discussed in appendix B, the spring constant may be written as (eq. (B10))

$$k = \frac{\gamma M_2}{1 - M_2} \left(\frac{c}{m} \right) \alpha \qquad (33)$$

The behavior of $m, c/\alpha$, and k/α^2 as functions of the upstream Mach number M_1 is shown in figure 3 for $\gamma = 7/5$. The characteristic behavior of equation (31) is governed by the damping ratio ς,

$$\varsigma = \frac{c}{2\sqrt{mk}} \qquad (34)$$

and the undamped natural frequency,

$$\omega = \sqrt{\frac{k}{m}} \qquad (35)$$

Since c is proportional to α, k is proportional to α^2. The spring coefficient k is, therefore, independent of the sign of α. The damping ratio ς, on the other hand, has the same sign as α, but is independent of the magnitude of α.

In general, the following five cases are recognized:

(1)	$\varsigma < 0$	Unstable
(2)	$\varsigma = 0$	Undamped
(3)	$0 < \varsigma < 1$	Underdamped
(4)	$\varsigma = 1$	Critically damped
(5)	$\varsigma > 0$	Overdamped

The behavior of ς for $\alpha > 0$ as a function of M_1 is plotted in figure 4. The local analysis predicts an underdamped behavior for the shock motion in the divergent section. As M_1 approaches infinity, ς approaches a value of 0.74. In the convergent section ($\alpha < 0$), the magnitude of ς is the same as that shown in figure 4; however, its sign is negative and, therefore, the shock is unstable. The behavior of the undamped natural frequency is shown in figure 5. The case $\alpha = 0$ corresponds to case (2), and the system is said to be undamped. However, for this case, the linear approximation does not meet the Liapunov criterion that F_z be nonzero. Thus, further analysis is required to make a conclusive statement about this case.
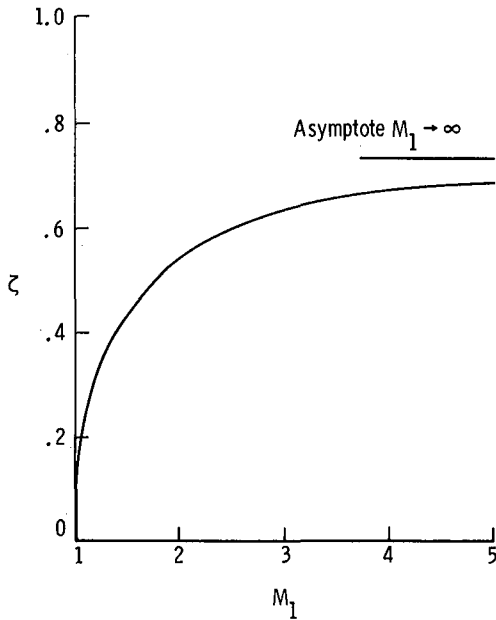

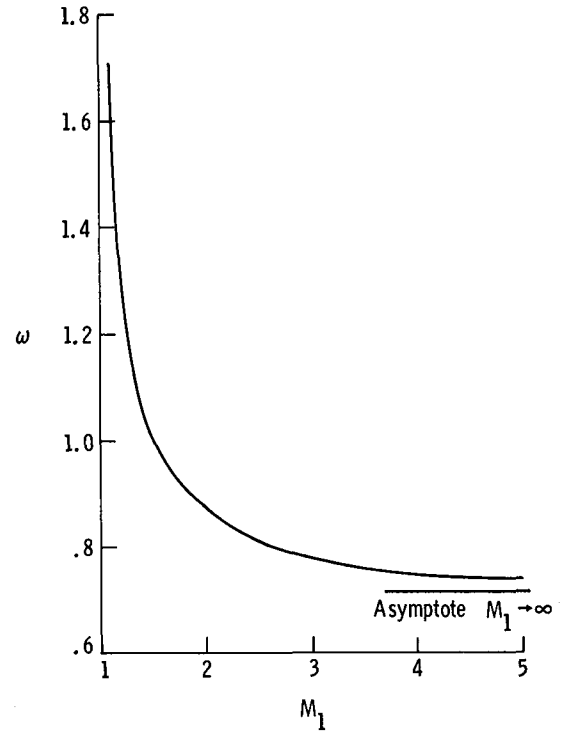Figure 4. Behavior of damping ratio ς as a function of M_1.

Figure 5. Behavior of undamped natural frequency ω as a function of M_1.

Nozzle Problem With Isentropic Shock

For weak shocks, it is generally accepted that the entropy generated at the shock can be neglected without seriously compromising the quality of the results. Under this approximation, the velocity field is described by the gradient of a potential function that satisfies the conservation of mass equation. The pressure and density are obtained by satisfying the conservation of energy equation and the isentropic pressure-density relation. For the nozzle problem illustrated in figure 1, the potential approximation to a shock connects the supersonic branch (curve abf) to the isentropic subsonic branch (curve agh). Therefore, there is an indeterminacy in the shock position, since a shock anywhere in the channel satisfies the imposed back pressure corresponding to point h in figure 1. The problem is discussed in detail in reference 9. The interest here is to examine the stability of such an isentropic shock which, in view of the above remarks, is expected to behave differently from the Rankine-Hugoniot shock just investigated.

For this problem, the governing equations are the time-dependent conservation of mass and energy equations and the isentropic pressure-density relation. With these equations, it is easy to show that once again equation (4) is valid along the left-running characteristic reaching the subsonic side of the shock. The jump relations across the shock are now given by

$$\rho_1\left(u_1 - w\right) = \rho_2(u_2 - w) \tag{36}$$

$$\frac{\gamma p_1}{\rho_1} + \delta(u_1 - w)^2 = \frac{\gamma p_2}{\rho_2} + \delta(u_2 - w)^2 \tag{37}$$

$$\frac{p_2}{p_1} = \left(\frac{\rho_2}{\rho_1}\right)^\gamma \tag{38}$$

from which, proceeding as before, one gets equations (15) and (16) but with P, Q, R, and S now defined as

$$P = \frac{\gamma M_2^2}{1 - M_2^2} \tag{39}$$

$$Q = -\frac{\gamma M_1}{(1 - M_2^2)\, a_1} \left(\frac{a_1}{a_2}\right)^2 \left[1 - \left(\frac{\rho_1}{\rho_2}\right)^2\right] \tag{40}$$

$$R = -\left(1 + \frac{P}{\gamma}\right) \tag{41}$$

$$S = \frac{\left(\frac{\rho_2}{\rho_1} - 1\right)}{M_1 a_1} - \frac{Q}{\gamma} \tag{42}$$

Now evaluating equation (4) at the shock results in an equation equivalent to equation (31), namely,

$$m\ddot{z} = 0 \tag{43}$$

where

$$m = \gamma M_2 S - Q \tag{44}$$

$$c = 0 \tag{45}$$

$$k = 0 \tag{46}$$

For the isentropic shock, the damping coefficient is identically zero. The shock is, therefore, undamped. However, like the Rankine-Hugoniot shock with $\alpha = 0$, the linear approximation fails the Liapunov criterion, and further analysis is required to study the effect of F on the solution. The isentropic and Rankine-Hugoniot mass coefficients are compared in figure 6.

Planar Shock Attached to a Wedge or Cone

For flow over a wedge or cone whose deflection angle is less than the angle associated with shock detachment for an incoming supersonic flow, the steady-state Euler equations admit two different solutions. The solutions are labeled according to the strength of the attached shock, which can be either strong or weak, depending upon whether its inclination is greater or less than the shock-wave inclination at detachment. The stability of
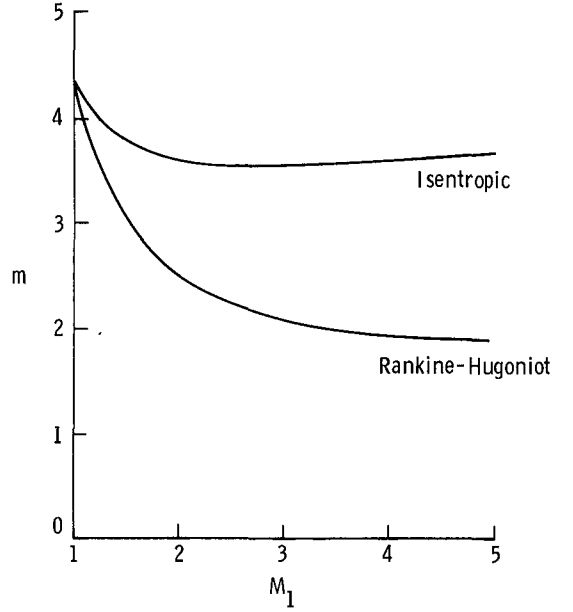
Figure 6. Comparison between isentropic and Rankine-Hugoniot mass coefficients as a function of M_1.
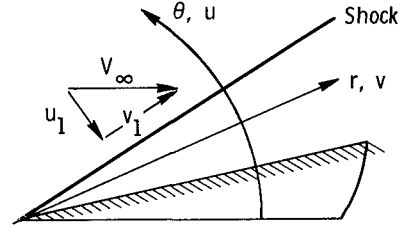
Figure 7. Diagram of coordinate system and velocity components used for shock attached to a wedge or cone.

these two solutions has been studied numerically in reference 5, to which the reader is referred for a derivation of the governing equations and other pertinent information. For the present purpose, one need consider only the compatibility relation reaching the shock on the high-pressure side, namely,

$$\frac{p_\tau}{p} + \gamma M \frac{u_\tau}{u} + \frac{\lambda^+ - w}{r_o} \left(\frac{p_\xi}{p} + \gamma M \frac{u_\xi}{u}\right) + \frac{\gamma}{r_o}\left[\lambda^+ \left(\frac{v}{a}\right) + (v + u\cot\theta)j\right] = 0 \tag{47}$$

where v and u are the radial and circumferential velocity components as indicated by figure 7; also, $j = 0$ for the two-dimensional flow over a wedge, and $j = 1$ for the axisymmetric flow over a circular cone. Equation (47) is valid on the left-running characteristic where

$$\lambda^+ = u + a \tag{48}$$

and where, as before, a frame of reference moving with the shock is used:

$$\left.\begin{array}{l} \tau = t \\ \xi = [\theta - \theta_s(t)]\, r_o \end{array}\right\} \quad (49)$$

Here $\theta_s(t)$ defines the shock-wave inclination, and $w = r_o\dot\theta_s$ is the shock-wave speed.

If one denotes by a subscript 1 conditions on the low-pressure side of the shock that depend on the shock location and by a subscript ∞ conditions on the low-pressure side that are constant, the free-stream Mach number is given by

$$M_\infty = \frac{\left(u_1^2 + v_1^2\right)^{1/2}}{a_\infty} = \frac{V_\infty}{a_\infty} \quad (50)$$

where

$$u_1 = V_\infty \sin\theta \quad (51)$$

$$v_1 = V_\infty \cos\theta \quad (52)$$

The component of the free-stream Mach number normal and relative to the moving shock is given by

$$M_1 = \frac{(u_1 - w)}{a_\infty} \quad (53)$$

The jump conditions relating the low-pressure side to the high-pressure side, denoted by subscript 2, are

$$v_1 - w = v_2 - w \quad (54)$$

$$\frac{p_2}{p_\infty} = \frac{\gamma M_1^2 - \delta}{\beta} \quad (55)$$

$$\frac{u_2 - w}{u_1 - w} = \frac{\delta M_1^2 + 1}{\beta M_1^2} \quad (56)$$

Proceeding as before, one gets equations (15) and (16) where $P, Q, R,$ and S are now defined as

$$P = \frac{2\gamma}{\beta}\left(\frac{p_\infty}{p_2}\right) M_\infty^2 \sin\theta \cos\theta \quad (57)$$

$$Q = \frac{2\gamma}{\beta}\left(\frac{p_\infty}{p_2}\right)\left(\frac{M_\infty \sin\theta}{a_\infty}\right) \quad (58)$$

$$R = \left[\frac{1}{\sin\theta} - 2\left(\frac{a_\infty}{a_2}\right)\left(\frac{M_\infty}{M_2}\right)\left(\frac{\delta}{\beta} - \frac{\rho_\infty}{\rho_2}\right)\right]\cos\theta \quad (59)$$

$$S = \frac{1}{u_2}\left[1 - \frac{\rho_\infty}{\rho_2} - 2\left(\frac{\delta}{\beta} - \frac{\rho_\infty}{\rho_2}\right)\right] \quad (60)$$

With $z = \theta_s - \theta_{s,0}$, the equation governing the motion of the shock is equation (31), where now

$$m = Q + \gamma M_2 S \quad (61)$$

$$c = P + \gamma M_2 R + \frac{T}{\lambda^+} \quad (62)$$

$$k = \frac{T}{\lambda^+}\left(\frac{c}{m}\right) \quad (63)$$

and

$$T = \frac{\gamma\lambda^+}{r_o}\left(\frac{v_2}{a_2} + j\frac{\frac{v_1}{a_2} + M_2\cot\theta}{M_2 + 1}\right) \quad (64)$$

The behavior of ς as a function of free-stream Mach number and shock-wave inclination is shown in figure 8 for $\gamma = 7/5$ and $r_o = 1$. As expected, the local analysis predicts that both weak and strong shocks are stable. This analysis, as already mentioned, does not include the effect of far-field boundary conditions which, according to reference 5, must be included to determine the overall stability of the problem. The behavior of the undamped natural frequency is shown in figure 9.

Conclusions

A procedure has been developed to study the local stability of planar shock waves. In general, the equation governing the shock motion is equivalent to the equation of a damped harmonic oscillator. For a Rankine-Hugoniot shock in a divergent-convergent nozzle, the analysis predicts a stable solution in the divergent section and an unstable solution in the convergent section, in agreement with well-known experimental observations. For an isentropic shock in a nozzle, the analysis predicts an undamped behavior. For shock waves attached to wedges and cones, it predicts a stable solution for both strong and weak shocks.

Langley Research Center
National Aeronautics and Space Administration
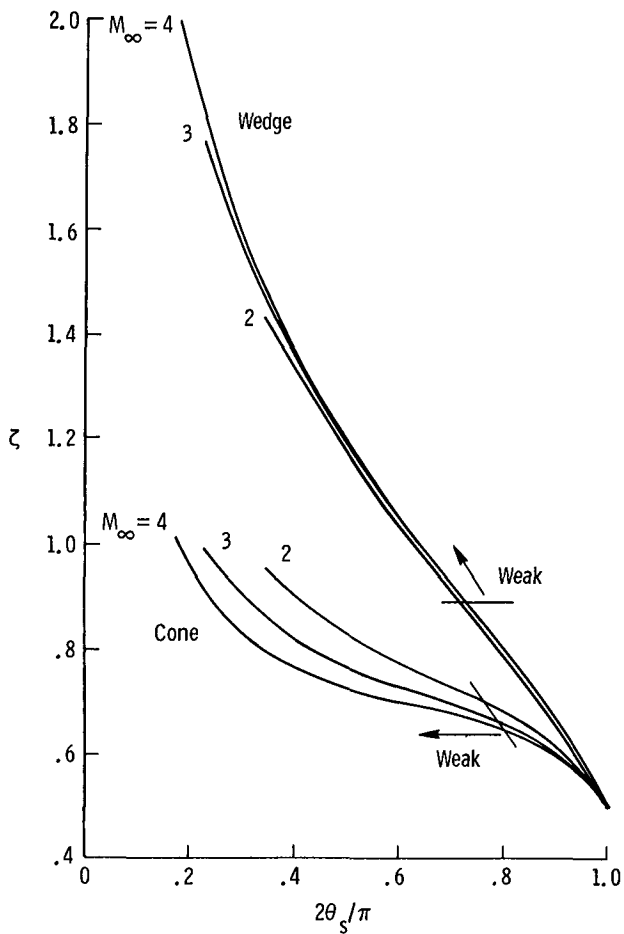Hampton, VA 23665
September 21, 1984

Figure 8. Behavior of damping ratio ζ for cones and wedges at $M_\infty = 2, 3$, and 4 as a function of the shock-wave inclination. $\gamma = 7/5; r_o = 1$.
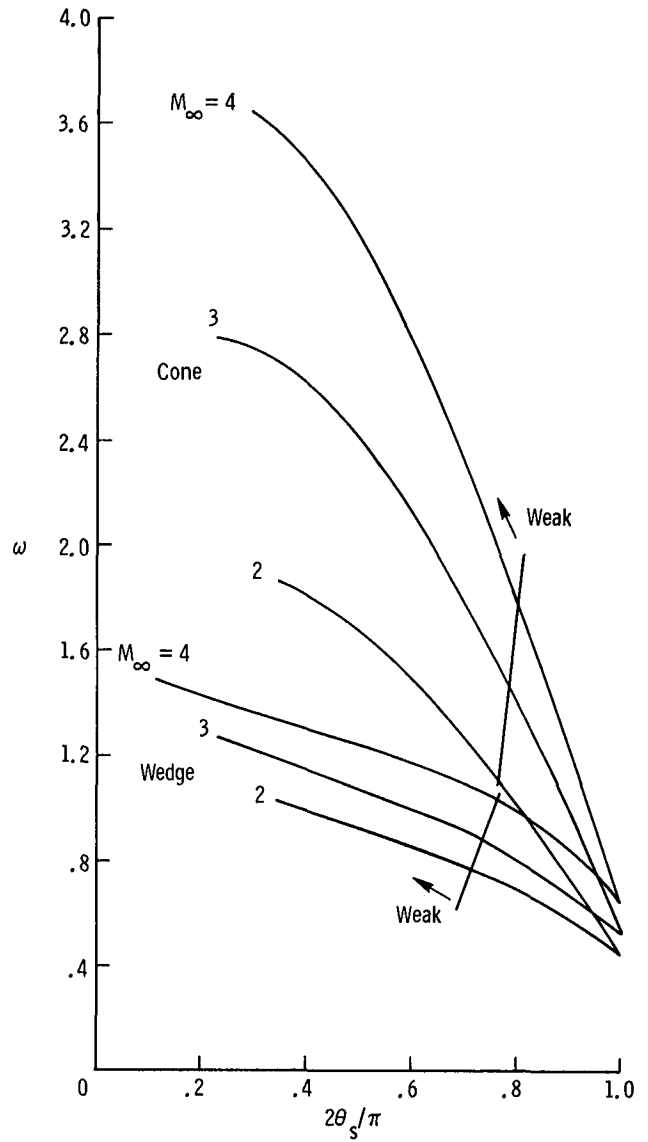

Figure 9. Behavior of undamped natural frequency ω for cones and wedges at $M_\infty = 2, 3$, and 4 as a function of the shock-wave inclination. $\gamma = 7/5; r_o = 1$.

Appendix A

Steady, Quasi-One-Dimensional Flow-Field Dependence On Area Variation

The following expressions are derived in reference 1:

$$\frac{dM}{M} = -\frac{1 + \delta M^2}{1 - M^2}\frac{dA}{A} \tag{A1}$$

$$\frac{du}{u} = -\frac{1}{1 - M^2}\frac{dA}{A} \tag{A2}$$

$$\frac{da}{a} = \frac{\delta M^2}{1 - M^2}\frac{dA}{A} \tag{A3}$$

$$\frac{d\rho}{\rho} = \frac{M^2}{1 - M^2}\frac{dA}{A} \tag{A4}$$

$$\frac{dp}{p} = \frac{\gamma M^2}{1 - M^2}\frac{dA}{A} \tag{A5}$$

At the shock, the following relation is also valid:

$$\frac{1}{A}\frac{dA}{d\tau} = \alpha w \tag{A6}$$

Appendix B

Evaluation of Spring Constant k

Equation (22) may be written as

$$F = \frac{\lambda^-}{p} (p_\xi - \rho a u_\xi) + \gamma u \alpha \qquad (B1)$$

Therefore,

$$F_\tau = \left(\frac{\lambda^-}{p}\right)_\tau (p_\xi - \rho a u_\xi) + \frac{\lambda^-}{p} (p_\xi - \rho a u_\xi)_\tau + (\gamma u \alpha)_\tau \qquad (B2)$$

From equation (4), it follows that

$$\left(p_\xi - a\rho u_\xi\right)_\tau$$
$$= -\frac{(p_\tau - \rho a u_\tau)_\tau + \left(\lambda^- - w\right)_\tau \left(p_\xi - \rho a u_\xi\right) + (\gamma p u \alpha)_\tau}{\lambda^- - w} \qquad (B3)$$

The term $(p_\tau - \rho a u_\tau)_\tau$ cannot be evaluated. However, in reference 10, it was shown for a number of problems similar to the one considered here that along the shock path, the term $(p_\tau - \rho a u_\tau)$ is approximately zero. Therefore, the first term in the right-hand side of equation (B3) is neglected. Substituting this equation in equation (B2) yields

$$F_\tau = \left\{ \left[\left(\frac{\lambda^-}{p}\right)_\tau - \left(\frac{\lambda^-}{p}\right) \frac{(\lambda^- - w)_\tau}{\lambda^- - w} \right] (p_\xi - \rho a u_\xi) - \left(\frac{\lambda^-}{p}\right) \frac{(\gamma p u \alpha)_\tau}{\lambda^- - w} + (\gamma u \alpha)_\tau \right\} \qquad (B4)$$

The above expression is to be evaluated at $\tau = 0$ on the subsonic side of the shock, denoted by subscript 2. From equation (B1), one has

$$(p_\xi - \rho a u_\xi) \,|_{2,0} = \left.\frac{-\gamma u p \alpha}{\lambda^-}\right|_{2,0} \qquad (B5)$$

and, therefore,

$$F_\tau|_{2,0} = \left.\frac{-\gamma u \alpha w_\tau}{\lambda^-}\right|_{2,0} \qquad (B6)$$

But, from equation (25) evaluated at $\tau = 0$, one gets

$$w_{\tau,0} = -\frac{c w_0}{m} \qquad (B7)$$

and, therefore,

$$F_\tau|_{2,0} = \frac{\gamma M_2}{M_2 - 1} \frac{c}{m} \alpha w_0 \qquad (B8)$$

Since,

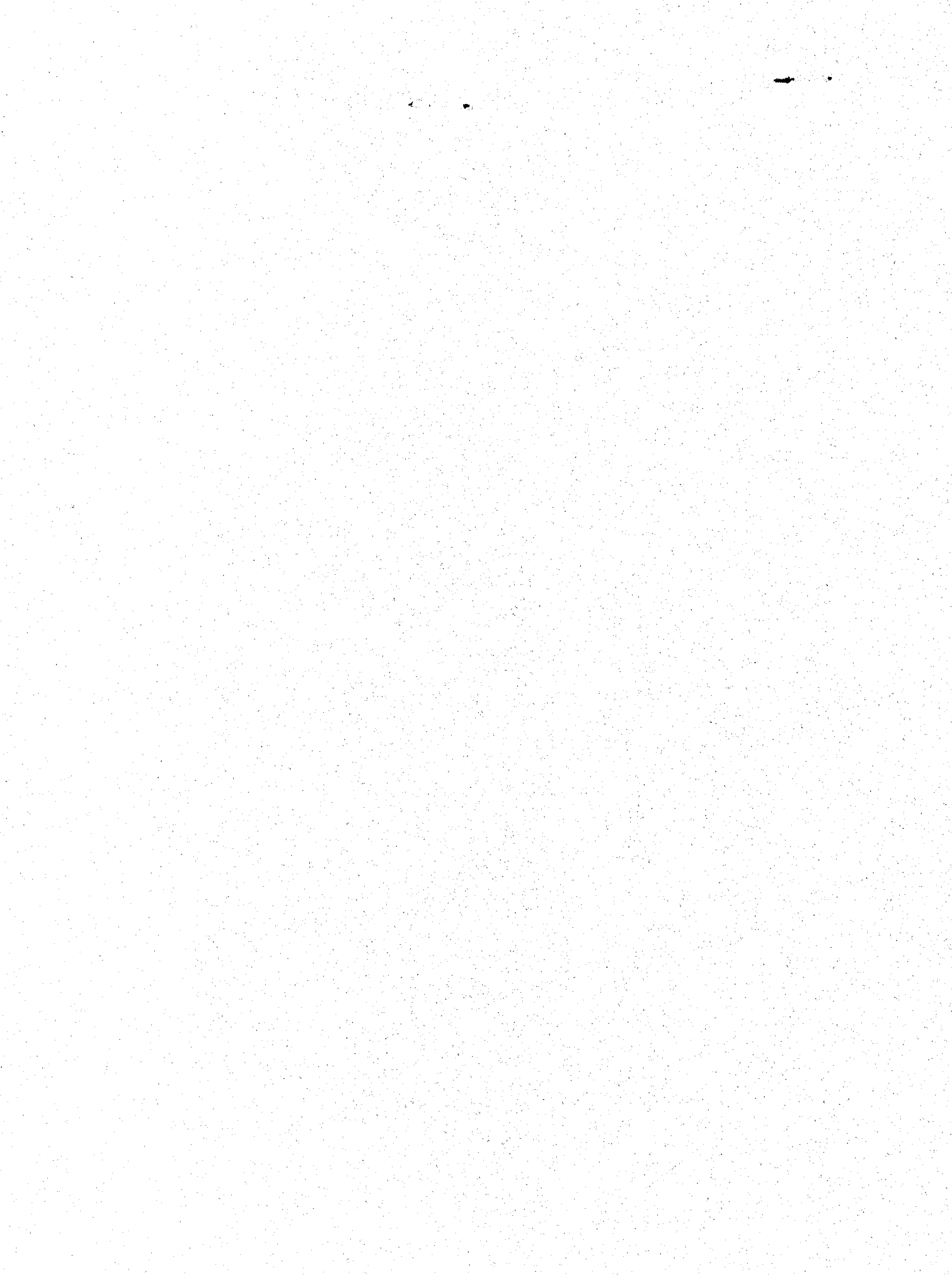$$F_z|_{2,0} = \frac{F_\tau|_{2,0}}{w_0} \qquad (B9)$$

the spring constant is given by

$$k = \frac{\gamma M_2}{1 - M_2} \frac{c}{m} \alpha \qquad (B10)$$

The spring constant for the wedge or cone problem, given by equation (63), can be evaluated in the same manner by replacing $\gamma u \alpha$ in equation (B1) by T and repeating the analysis.

References

1. Shapiro, Ascher H.: *The Dynamics and Thermodynamics of Compressible Fluid Flow. Volume I.* Ronald Press Co., c.1953, pp. 146, 228.

2. Kantrowitz, Arthur: *The Formation and Stability of Normal Shock Waves in Channel Flows.* NACA TN 1225, 1947.

3. Moretti, Gino: *Complicated One-Dimensional Flows.* PIBAL Rep. No. 71-25 (Contract No. DAHC04-69-C-0077), Dep. Aerosp. Eng. & Appl. Mech., Polytech. Inst. of Brooklyn, Sept. 1971. (Available from DTIC as AD 731 494.)

4. Culick, F. E. C.; and Rogers, T.: The Response of Normal Shocks in Diffusers. *AIAA J.,* vol. 21, no. 10, Oct. 1983, pp. 1382–1390.

5. Salas, M. D.; and Morgan, B. D.: Stability of Shock Waves Attached to Wedges and Cones. *AIAA J.,* vol. 21, no. 12, Dec. 1983, pp. 1611–1617.

6. Minorsky, N.: *Introduction to Non-Linear Mechanics.* J. W. Edwards (Ann Arbor, Mich.), 1947, pp. 48–55.

7. Slater, John C.; and Frank, Nathaniel H.: *Mechanics.* McGraw-Hill Book Co., Inc., 1947, pp. 21–29.

8. Greenwood, Donald T.: *Principles of Dynamics.* Prentice-Hall, Inc., c.1965, pp. 97–104.

9. Deconinck, H.; and Hirsch, Ch.: Boundary Conditions for the Potential Equation in Transonic Internal Flow Calculation. ASME Paper 83-GT-135, Mar. 1983.

10. Whitham, G. B.: On the Propagation of Shock Waves Through Regions of Non-Uniform Area or Flow. *J. Fluid Mech.,* vol. 4, pt. 4, Aug. 1958, pp. 337–360.

1. Report No. NASA TP-2387	2. Government Accession No.	3. Recipient's Catalog No.
4. Title and Subtitle LOCAL STABILITY ANALYSIS FOR A PLANAR SHOCK WAVE		5. Report Date December 1984
		6. Performing Organization Code 505-31-03-01
7. Author(s) M. D. Salas		8. Performing Organization Report No. L-15768
9. Performing Organization Name and Address NASA Langley Research Center Hampton, VA 23665		10. Work Unit No.
		11. Contract or Grant No.
12. Sponsoring Agency Name and Address National Aeronautics and Space Administration Washington, DC 20546		13. Type of Report and Period Covered Technical Paper
		14. Sponsoring Agency Code

15. Supplementary Notes

16. Abstract

A procedure is presented to study the local stability of planar shock waves. The procedure is applied to a Rankine-Hugoniot shock in a divergent-convergent nozzle, to an isentropic shock in a divergent-convergent nozzle, and to Rankine-Hugoniot shocks attached to wedges and cones. For each case, the equation governing the shock motion is shown to be equivalent to the damped harmonic oscillator equation.

17. Key Words (Suggested by Authors(s)) Stability analysis Shock waves Nozzle flows	18. Distribution Statement Unclassified—Unlimited Subject Category 02

19. Security Classif.(of this report) Unclassified	20. Security Classif.(of this page) Unclassified	21. No. of Pages 12	22. Price A02

National Aeronautics and
Space Administration

Washington, D.C.
20546

THIRD-CLASS BULK RATE

LANGLEY RESEARCH CENTER

3 1176 00189 6266

U.S.MAIL

NASA